

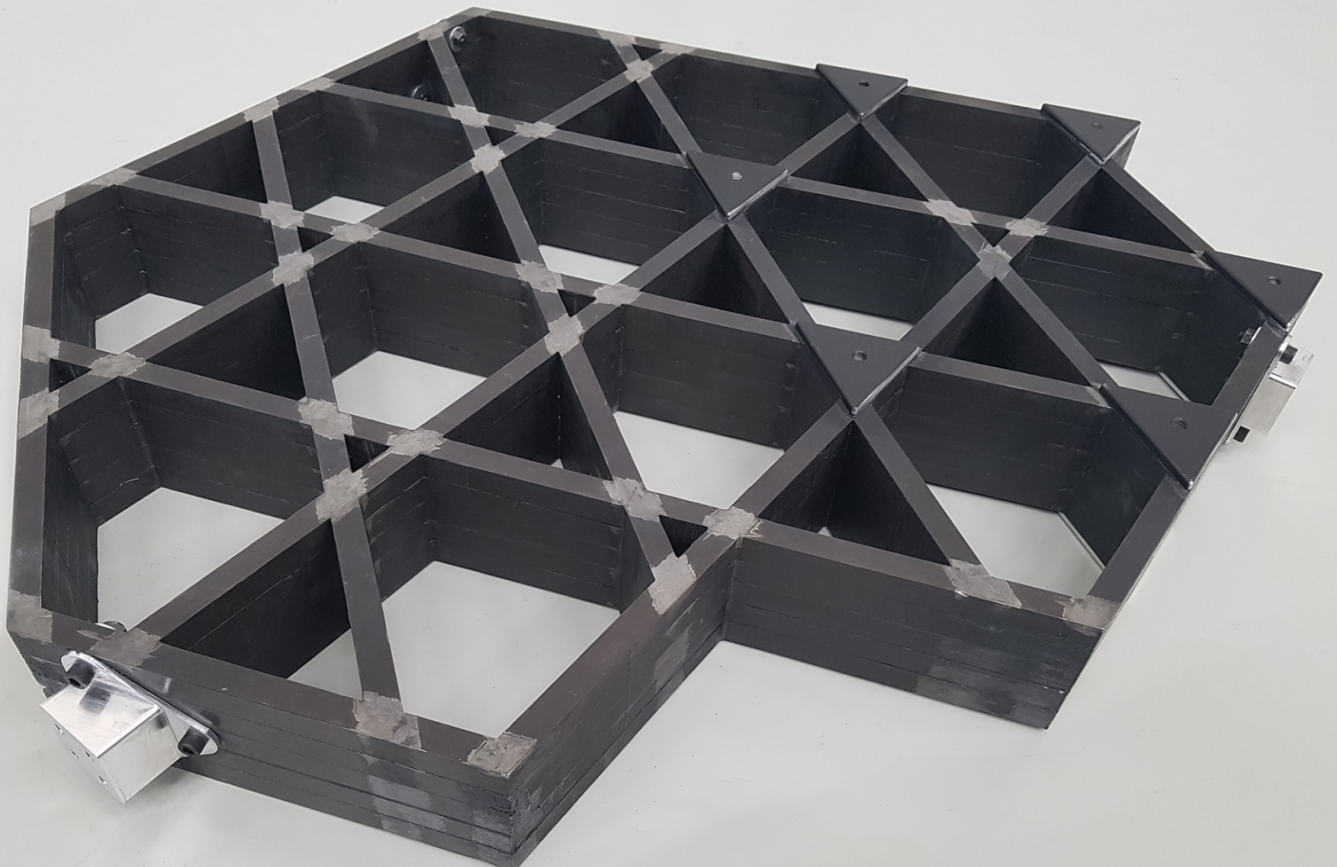


Dedicated to innovation in aerospace

NLR-TP-2019-346 | May 2020

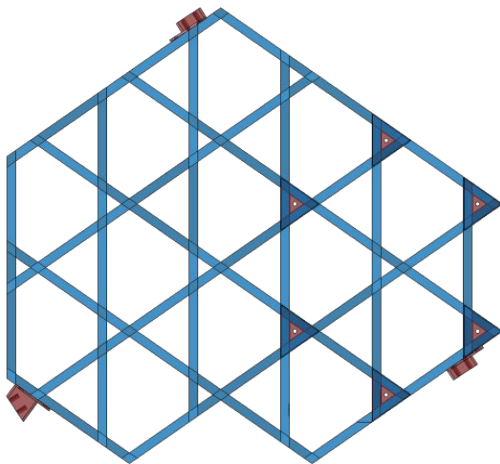
Dimensionally Stable CFRP Grid Stiffened Structures for Space Applications

CUSTOMER: European Space Agency



NLR – Royal Netherlands Aerospace Centre

Dimensionally Stable CFRP Grid Stiffened Structures for Space Applications



Problem area

Grid structures have already found aerospace applications using traditional materials such as aluminium from the Vickers Wellington bomber in the 1930's to the Delta launcher rockets in the 1980's. Composites and their automated production processes have revamped the interest in grid structures, as their anisotropy and different production process make them more efficient than in large scale aluminium aerospace structures.

Most current experimental applications are found in cylindrical structures, where filament winding of the entire grid at once is the most used production process. This is a relatively fast production process with in general lower laminate quality as compared to prepreg fiber placement. At the crossings, the overlapping layers lead to a local increase in thickness and fibre undulation which affects compression properties. If the thickness of the grid must be uniform the crossings need to be compacted giving higher fiber volume content at these locations compared to the rest of the grid. Examples are a fuselage section of the Ilyushin 114 and the Scaled Composites Visionaire Vantage.

REPORT NUMBER

NLR-TP-2019-346

AUTHOR(S)

S. Sterk
W.M. van den Brink

REPORT CLASSIFICATION

UNCLASSIFIED

DATE

May 2020

KNOWLEDGE AREA(S)

Structures and
Manufacturing Technology
Aerospace Materials
Aerospace Structures
Testing

DESCRIPTOR(S)

Composite
Grid
Fibre placement
Dimensionally stable

Description of work

In this paper, a flat grid without a skin is under consideration making filament winding a less convenient and less obvious choice. Furthermore, in contrast to the mainly in-plane loaded circular grid structures the flat grid will have high loading in the transverse direction on the grid. This work is carried out with funding and guidance from the European Space Agency with the main objective of the project to design, build and test a flat shaped dimensionally stable CFRP grid stiffened lattice structure to carry payloads in a space structure. A technical demonstrator will be built and tested, increasing the readiness of the technology to TRL 4.

Results and conclusions

A CFRP grid structure was developed to explore the capabilities and possibilities for use in future flat support structures with high dimensional stability requirements. The final design consists of an 80 mm high anisogrid type of design which has identical crossings and close to symmetric layout with metal inserts for payload and bipod interfaces. The final weight is 13.7 kilogram. It does not meet all the stability requirements set for the gravity release load case but by using a higher grid (90 mm) or stiffer fibres this should be achievable.

Automated Fibre placement of UD prepreg tapes followed by autoclave consolidation was used to manufacture the grid. A specific cutting sequence was used for the elements and the grid to avoid local thickness increase at the crossings while still having continuous fibres across the nodes in each layer.

The correlation between FEM and test displacements was within 8 %. However due to the small displacements the results are very sensitive to errors and accuracy of the displacement measurements during the test and high sensitivity towards the boundary conditions. The desired TRL level 4 has been achieved successfully. This activity demonstrates that CFRP based grid structures are a feasible solution for stable structure requirements.

Applicability

The results can be applied in all types of composite grid structures (circular, flat including skins) and grid layouts (orthogrid, isogrid, anisogrid) and is not limited to stiffness dominant structures only.

GENERAL NOTE

This report is based on a presentation held at the SAMPE Europe Conference, Nantes - France, 19 September 2019.

NLR

Anthony Fokkerweg 2

1059 CM Amsterdam, The Netherlands

p) +31 88 511 3113

e) info@nlr.nl i) www.nlr.nl



Dedicated to innovation in aerospace

NLR-TP-2019-346 | May 2020

Dimensionally Stable CFRP Grid Stiffened Structures for Space Applications

CUSTOMER: European Space Agency

AUTHOR(S):

S. Sterk

NLR

W.M. van den Brink

NLR

This report is based on a presentation held at the SAMPE Europe Conference, Nantes - France, 19 September 2019.

The contents of this report may be cited on condition that full credit is given to NLR and the authors.

This publication has been refereed by the Advisory Committee AEROSPACE VEHICLES (AV).

CUSTOMER	European Space Agency
CONTRACT NUMBER	4000110652/14/NL/SW
OWNER	NLR + partner(s)
DIVISION NLR	Aerospace Vehicles
DISTRIBUTION	Unlimited
CLASSIFICATION OF TITLE	UNCLASSIFIED

APPROVED BY:		Date
AUTHOR	S. Sterk	05-06-2020
REVIEWER	W. Gerrits	05-06-2020
MANAGING DEPARTMENT	H.G.J.S. Thuis	05-06-2020

Contents

Abbreviations	4
Abstract	5
1 Introduction	5
2 Design of dimensionally stable grid	6
2.1 Redesign for Mmufacturing	8
2.2 Detailed Design	9
3 Manufacturing and Testing	11
4 Conclusions	15
5 Acknowledgements	15
6 References	15

Abbreviations

ACRONYM	DESCRIPTION
CFRP	Carbon Fibre Reinforced Plastic
CME	Coefficient of Moisture Expansion
CTE	Coefficient of Thermal Expansion
DIC	Digital Image Correlation
ESA	European Space Agency
FE	Finite Element
FEM	Finite Element Method
NLR	Royal Netherlands Aerospace Centre
RTM	Resin Transfer Moulding
SWIR	Short-Wave-Infrared
TRL	Technology Readiness Level
TROPOMI	Tropospheric Monitoring Instrument
TSS	Telescope Support Structure
UD	Uni-Directional
UVN	Ultra-violet Visible and Near Infrared (Light Imaging Spectrometer)

DIMENSIONALLY STABLE CFRP GRID STIFFENED STRUCTURES FOR SPACE APPLICATIONS

Senne Sterk, Wouter van den Brink
Royal Netherlands Aerospace Centre
Voorsterweg 31
Marknesse 8316 PR

ABSTRACT

The main objective of the project is to design, build and test a flat shaped dimensionally stable CFRP grid stiffened lattice structure to carry payloads in a space structure. The project is divided in three phases: Phase 1 is for selection of target applications, requirements and materials and processes, phase 2, is for the detail design and optimization of the intended grid structure and phase 3 is for the manufacturing and mechanical testing of the technical demonstrator. The preliminary design is compared to a chosen baseline application. A coupon and element level test program will provide the material properties specific for the chosen process and design features. The final technology readiness is TRL 4.

1. INTRODUCTION

Grid structures have already found aerospace applications using traditional materials such as aluminium from the Vickers Wellington bomber in the 1930's to the Delta launcher rockets in the 1980's. Composites and their automated production processes have revamped the interest in grid structures, as their anisotropy and different production process make them more efficient than in large scale aluminium aerospace structures.

Most current experimental applications are found in cylindrical structures, where filament winding of the entire grid at once is the most used production process [1]. This is a relatively fast production process with in general lower laminate quality as compared to prepreg fiber placement. Due to the tension in the winding fiber around the mostly circular mould, the material is compacted. At the crossings, the overlapping layers lead to a local increase in thickness and fibre undulation which affects compression properties. If the varying thickness is not an issue in the final product more room is taken into account in the tool to accommodate the extra fibers. If the thickness of the grid must be uniform the crossings need to be compacted giving higher fiber volume content at these locations compared to the rest of the grid. Examples are a fuselage section of the Ilyushin 114 and the Scaled Composites Visionaire Vantage [1].

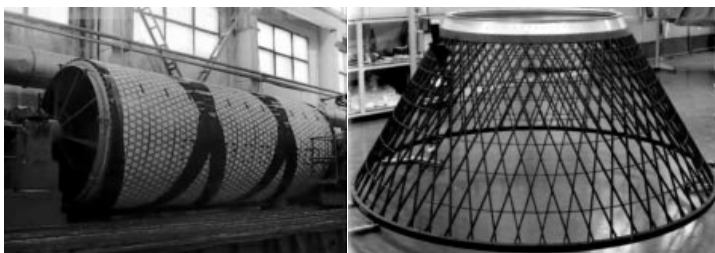


Figure 1: Examples of filament wound launcher grid structures [1]

In this paper, a flat grid without a skin is under consideration making filament winding a less convenient and less obvious choice. Previous examples exist of fiber placed grid structures, for instance in the TowOpt [2] and ICARO [3] projects. Furthermore, in contrast to the mainly in-plane loaded circular grid structures the flat grid will have high loading in the transverse direction on the grid. With that in mind, high and narrow grids will be used because of their high bending stiffness. In order to achieve those high and narrow grids, the fiber placement machine will be used with only one or two tows.

This work is carried out with funding and guidance from the European Space Agency with the main objective of the project to design, build and test a flat shaped dimensionally stable CFRP grid stiffened lattice structure to carry payloads in a space structure. A technical demonstrator will be built and tested, increasing the readiness of the technology to TRL 4.

2. DESIGN OF DIMENSIONALLY STABLE GRID

In the early stages of the project the Telescope Support Structure (TSS) of TROPOMI was selected for the application of a dimensionally stable CFRP grid structure. The Tropospheric Monitoring Instrument (TROPOMI) is an Earth-viewing imaging spectrograph that consists of two optical modules, namely the UVN and the SWIR. The design concept is based on an aluminium sandwich base plate with three Kinematic Mounts. The two optical modules are attached to the base plate and require an accurate relative positioning of both. A picture of the TROPOMI TSS is shown in Figure 2.

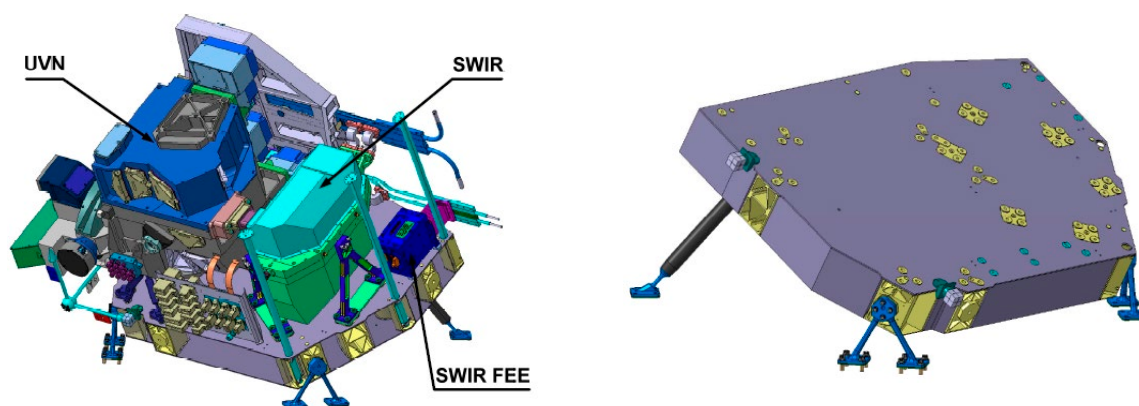


Figure 2: Overview of the TROPOMI instrument (left) and TSS base plate (right) Source: Airbus DS NL

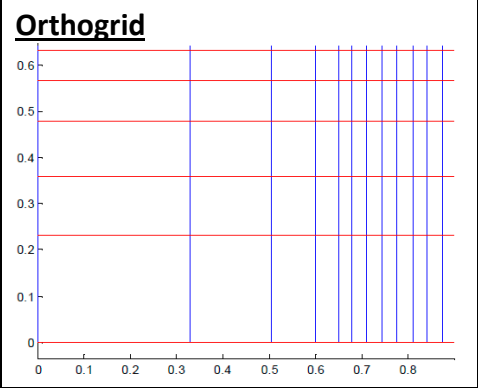
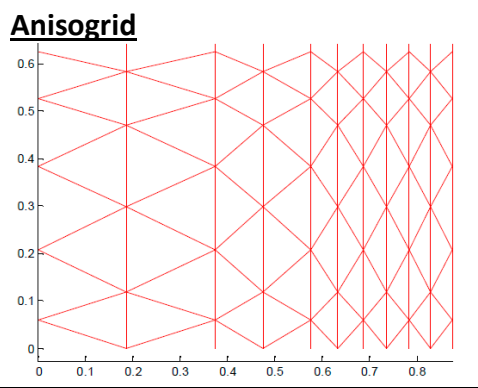
For the preliminary design phase the mechanical stability of the TSS base plate was analyzed by FEM to serve as a reference for the CFRP grid. The stability of the TSS baseplate was investigated for gravity release and a temperature gradient. In orbit, the release of the gravity load will lead to the relief of deformation and result in a distortion of the instrument positions. The analyses showed that the baseplate met the requirements for gravity release.

The first step for the preliminary design was to make a down-selection of materials, process and candidate grid geometries with a focus on dimensional stability. On the material side, this means that fibres with high stiffness and low coefficient of thermal expansion (CTE) must be combined with a matrix with low CTE/CME. Cyanate esters such as Hexcel 954-3, Solvay HTM110, or Ten Cate RS-3 are good candidates for prepreg fibre placement with the M55J or M46J high modulus fibres. As a fall-back position an epoxy resin system (Solvay 977-6) was also considered. Fibre placement of prepreg or dry tapes combined with autoclave cure or a RTM injection process respectively are the most suitable manufacturing methods. The grid geometries considered are orthogrid and (an)isogrid designs.

The preliminary design was conducted in two phases. In the first phase, the TSS base plate is approximated as a rectangle and an optimization scheme based on a parametrised cell is used to determine the lightest weight configuration under gravity release and thermal loads. In the second phase, the best design from the rectangular base plate is superimposed onto the exact footprint of the TROPOMI base plate. Then, a detailed finite element (FE) model using shell elements is used to tweak the design on the basis of mechanical, thermal and moisture loading as well as launch loads. In the analyses only the SWIR payload was taken into account. Geometry post-processing was used to retrieve discrete stiffener paths for the preliminary design. Slight changes of stiffener spacing's in the geometry post-processing are possible in order to make sure that grid intersections match the payload attachment points and the three attachment points for the entire base plate.

During the first phase manufacturing constraints for the fibre placement process were taken into account. The main constraints are the minimum tape length the fibre placement machine can place (100 mm, corresponds to a minimum grid spacing of 50 mm) and the fact that the width of the grid members will have to be a multiple of ¼" as that is the width of the tows used in the fibre placement machine. A comparison between the orthogrid and anisogrid designs with a rib width of two tapes of the M55J fibre is shown in Table 1. Both designs are optimised for a weight target of 20 kg (excluding attachments) which is below the program requirement of 25 kg.

Table 1: Orthogrid versus anisogrid design

	Orthogrid	Anisogrid
		
Rib Width (mm)	12.7	12.7
Rib height (mm)	90.1	64.2
Min. rib spacing (mm)	32.7	46.2

The orthogrid design requires very short spacing values around the payload attachment of approximately 33 mm which is prohibitively low. The spacing of the anisogrid design is somewhat low in the vicinity of the payload attachment as well but close to the minimum grid spacing requirement of 50 mm. As a result, the orthogrid configuration was abandoned and optimization focused on the isogrid design.

In the second phase of the optimization the anisogrid design from the rectangular base plate was superimposed onto the exact footprint of the TSS base plate. Also, the final selection on the material was made during this phase as complete FE models of the baseplate were used on which the thermal, mechanical, and moisture loads could be applied. The optimization was

done by minimizing the weight while enforcing the constraints that the grid does not exceed a pre-selected height (70 mm) and the displacement and rotations of the payload attachment points do not exceed the requirements.

M46J/977-6 was chosen for the final design as going from M55J to the M46J fibre gives an increase of approximately one kg (~14 kg for M55J and ~15 kg for M46J) which is comfortably below the program target of 25 kg. Furthermore, the cost of the M55J fibre is approximately twice that of the M46J fibre. The stability due to moisture uptake by the resin was found to be well within requirements for both the cyanate-ester and epoxy resins. As the epoxy resins have a much better availability these resin systems were the preferred matrix material.

Using the M46J/977-6 material and the effect of the bipod attachments, the design was further refined in order to meet all the gravity release requirements. To minimize the deflections and rotations with the bipods present, three ribs connecting the attachment points of the baseplate with twice the nominal rib width needed to be added. The final design is shown in Figure 3. For the thermal load cases all requirements were met. Stresses for all loading conditions are low and not a concern in the design as it is stiffness dominated.

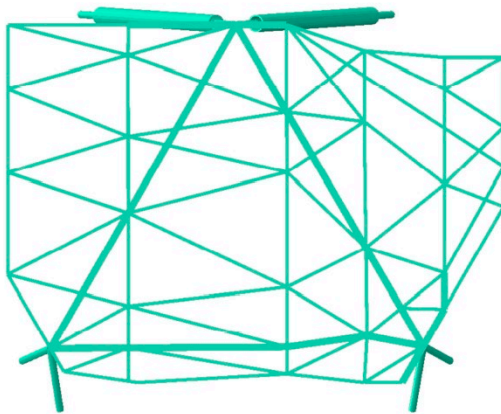


Figure 3: Final design resulting from preliminary design phase

Fiber	M46J
Matrix	977-6
Grid pattern	Anisogrid
Grid height (mm)	70
Grid width (mm)	6.35 ⁽¹⁾
Weight –baseplate only (kg)	15.2

⁽¹⁾ Equals the width of one tow of material. Note that some grid members are currently stiffened by increasing their width to two tows, 12.7 mm.

2.1 Redesign for manufacturing

Despite taking into account the most important manufacturing limitations the design from the preliminary design phase was too complex due to the varying rib width, crossings of three ribs or more and rib lengths close to the minimum rib spacing requirement. Furthermore, to prevent overlapping tapes, the non-perpendicular angles between the ribs create gaps between crossing tapes as the fibre placement machine can only cut the tapes perpendicular. The size of the gaps depends on the degree of the angle between the tape; a smaller angle creates larger gaps and vice versa. Another issue comes from the fact that most ribs constantly change their orientation after crossing another rib. This means that steering of the tapes would be needed to keep continuous fibres across the crossings. Another solution is to cut the fibres at the crossing and start at the new orientation of the next rib. Both options were not found to be acceptable. Small gaps are considered acceptable as the effect it has on stiffness is negligible [4].

The evolution of the design towards a manufacturable grid is shown in Figure 4. Additional constraints used were uniform rib width, completely straight ribs and a maximum of two ribs crossing in the same location. Initially, the outer contour of the TSS base plate was respected.

As can be seen on the left picture in Figure 4 the rib length near the outer contour was below the manufacturing constraint defined. Further rearrangement of the ribs could not solve this issue so it was decided to release the outer contour requirement and move towards a generic and more symmetrical design which can be taken as a reference for future CFRP grid baseplate designs. An intermediate layout is shown in the middle picture of Figure 4 and the final design is shown in the right picture.

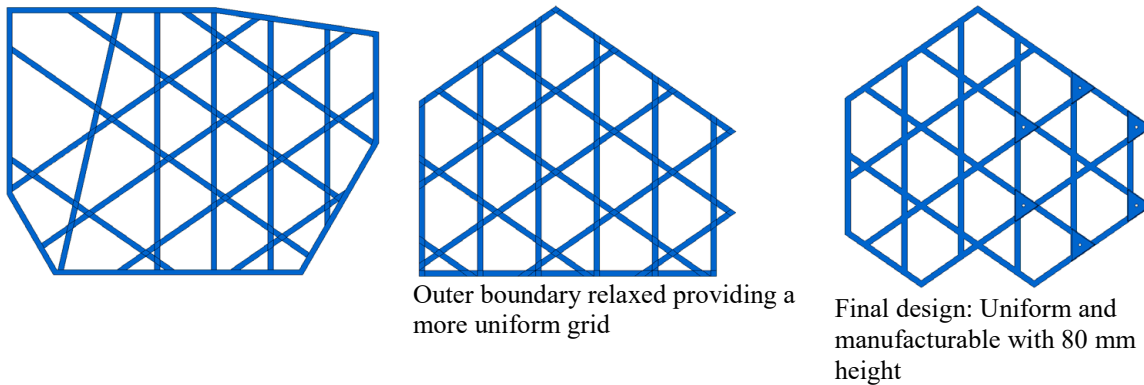


Figure 4: Evolution of design towards a manufacturable grid

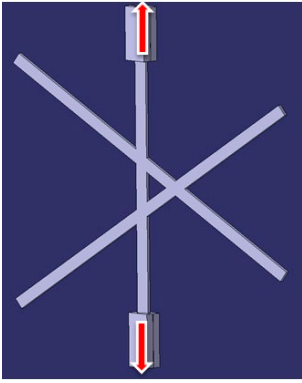
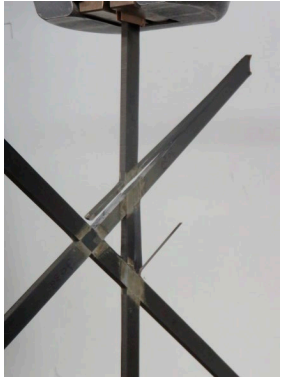
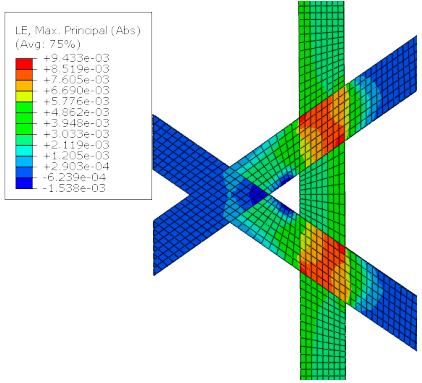
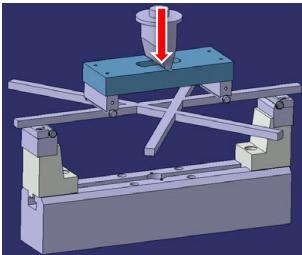
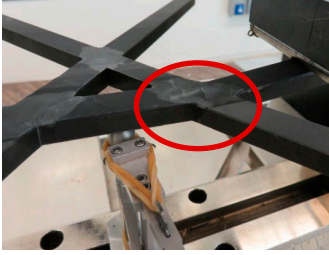
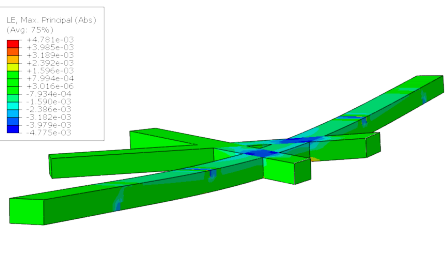
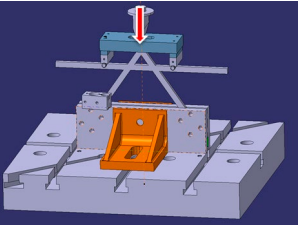
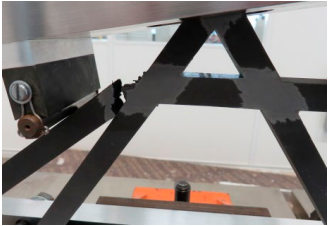
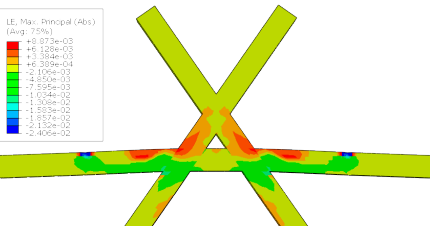
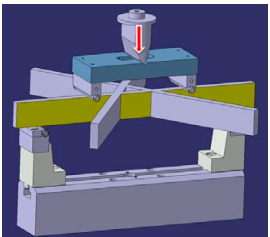
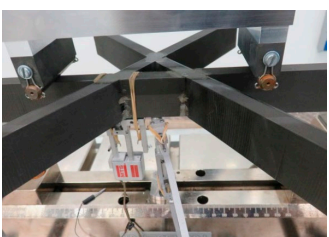
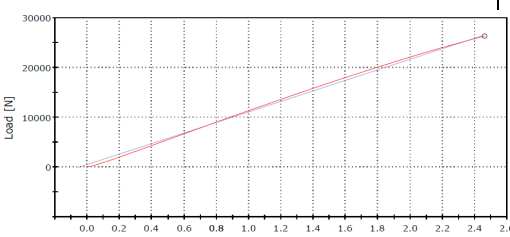
A final adjustment compared to the optimal geometry from the preliminary design phase was to move towards another material due to availability issues of M46J/977-6. A similar and available material was acquired from Hexcel being HM-63/M56 UD prepreg tape.

2.2 Detailed Design

To move towards the final detailed design a test programme on coupon and element level was carried out. The mechanical properties from coupon testing were used as input in Finite Element (FE) models of the elements and the entire grid. The element tests are used to compare the default way of modelling in the FE models (using volume 3D elements) to the experimental results.

Sixteen element level specimens including features from the final design shown in Figure 4 were tested under different loading conditions to verify the performance of the parts as manufactured. A comparison between the measured stiffness and the predicted stiffness is given in Table 2. The failure modes are also compared to the predictions, verifying that the model can accurately predict the failure locations on the tested specimens. More importantly, the simulated stiffness is a close match to the measured stiffness during the tests which demonstrates that the modelling approach is suitable to be used for the detailed design of the grid as well. Only for the 40 mm thick element the difference between the experiment and the prediction is larger. This was partly caused by local damage at the load introduction points due to the required force for sufficient displacement. A higher thickness to span ratio would be needed to prevent damage. Also the quality of the element was lower than desired due to insufficient gap impregnation which can also reduce the achieved specimen stiffness.

Table 2: Correlation of test data and numerical predictions

Type	Experiment stiffness	Simulation stiffness	Test vs. FEM
Tension	9.98 N/microstrain	9.51 N/microstrain	+4.9 %
  			
4pt bending	282 N/mm	277 N/mm	+1.8 %
  			
Vertical bending	8949 N/mm	8916 N/mm	+0.4 %
  			
4pt bending 40 mm	11026 N/mm	12621 N/mm	-12.6 %
  			

For the final detailed design the results from the coupon and element tests were incorporated into the FE model of the grid. In Figure 5 the final design of the grid and the inserts are shown and a summary of the most important characteristics is given.

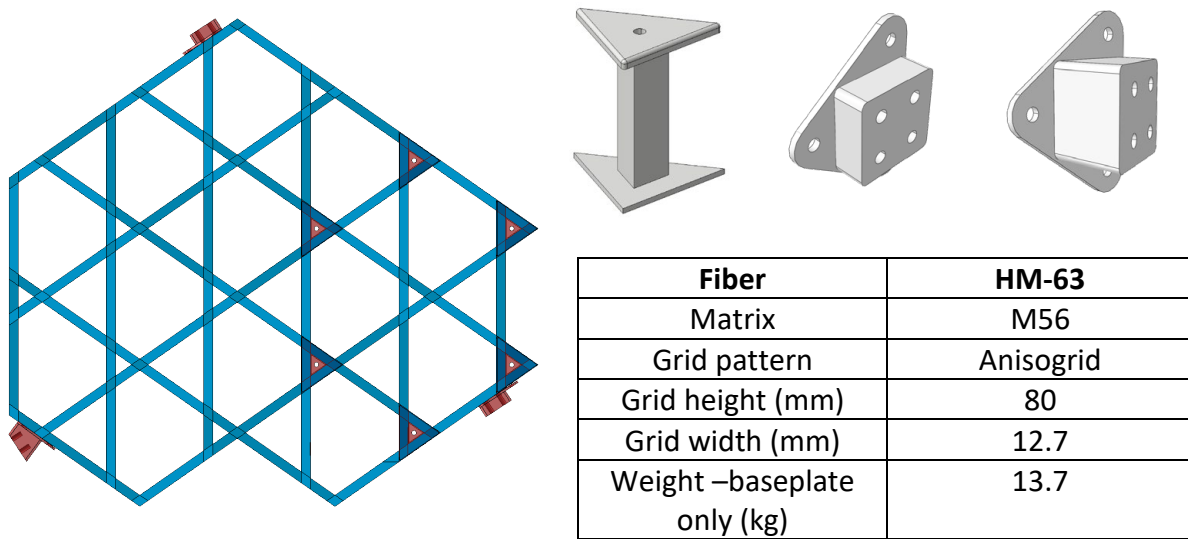


Figure 5: Final Design of the technical demonstrator and inserts. SWiR insert (left), flat bipod insert (middle) and angled bipod insert (right)

A consequence of releasing the TSS base plate as a reference and focus on future applications of a dimensionally stable CFRP grid structure was that the requirements defined earlier in the project were released as well and used only as a guideline. Similar to the initial preliminary design, gravity release is the only load case in which some rotations and displacements are not within the requirements. Two possible modifications that would enable full compliance with the requirements are to increase the height of the grid to 90 mm and/or use stiffer fibres. For the purpose of the project increasing the height did not add value to the demonstration of the technology and so the final height of the grid was kept at 80 mm. From the strength analyses no failure or damage is predicted for the design launch loads. Regarding the dimensional stability of the grid under thermal loads and moisture uptake all requirements are met.

3. MANUFACTURING AND TESTING

One of the challenges in manufacturing a CFRP grid is to deal with the deviating thickness at the crossing if all fibres are kept continuous. In TowOpt [2] two possibilities for the grid crossings were already investigated. To prevent thickness build-ups in the crossings, the fibers can be cut alternately or steered towards the sides, see Figure 6. Steering was not considered a viable option due to the high modulus fibres and relative short distance between the ribs. The alternating cutting option in combination with two tapes across the width of the ribs gives an interesting possibility to keep 50 % of the fibres in each layer continuous across the node. For a single tape only 50 % of the fibres of half of the layers are continuous. This is achieved by placing to two tapes continuous across the node and by cutting the other two tapes such that a temporarily gap is left next to the overlapping tapes. In the following layer the overlap and gap are interchanged and the thickness at the crossing is equal to the thickness of the ribs. In Figure 6 a picture is shown of the first layer for three ribs using the alternating cutting sequence. In this picture it is also clear that small triangular gaps remain between crossing tapes due to the inability of the fibre placement machine to cut at an angle.

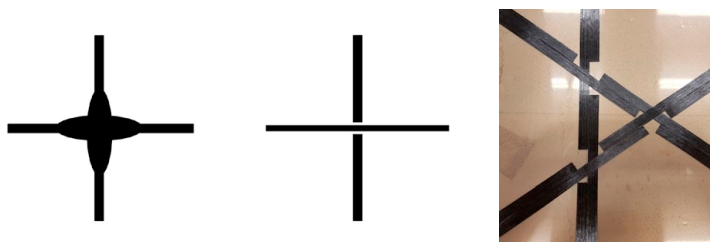


Figure 6: Steering at grid crossing (left), cutting with one tape (middle) and cutting with two tapes (right)

During manufacturing of the elements it was found that the small triangular gaps are not completely filled with resin which creates voids. Effort was put into the curing cycle to improve the impregnation of the gaps but was not successful. A solution was found in adding resin film patches at the crossings which compensates the missing material at the gaps and increases pressure at the nodes thus improving quality and impregnation. In Figure 7 two pictures of a cross-section are shown with and without the resin film patches. A clear improvement is seen and for the grid resin film patches were also used at all crossings.

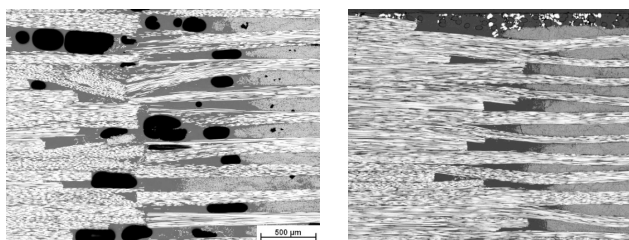


Figure 7: Cross-section of elements without resin patch (left) and with resin patch (right)

Another lesson learned from element manufacturing was that using the resin film patches and improved cure cycle worked successful to 20 mm thick elements. A 40 mm thick element which was manufactured showed incomplete impregnation of the gaps. Based on this result and to reduce the risk in manufacturing an 80 mm thick grid structure it was decided to divide the grid into five separate sections which are cured individually and bonded afterwards in a separate step together with the inserts. Bonding the sections will affect the stiffness and numerical analyses showed that 4 % stiffness was lost due to the effect of the bond lines. For the bonding 3M DP490 black was used in combination and the bond line was also incorporated in the FE models. The loss in stiffness was found acceptable and, if needed, can be compensated for by increasing the height of the grid at a minor weight penalty.

Each of the five sections was composed of two 10 mm thick preforms placed by the fibre placement machine. Due to the minimum tape length and start/stop runout the ribs in the preforms run outside the perimeter of the grid. Excessive material is removed manually before curing. Aluminium tool blocks and steel caul plates and edge dams were used to cure the five grid sections in an autoclave. Pictures of the manufacturing process are shown in Figure 8. The final assembled grid with inserts is shown in Figure 9.

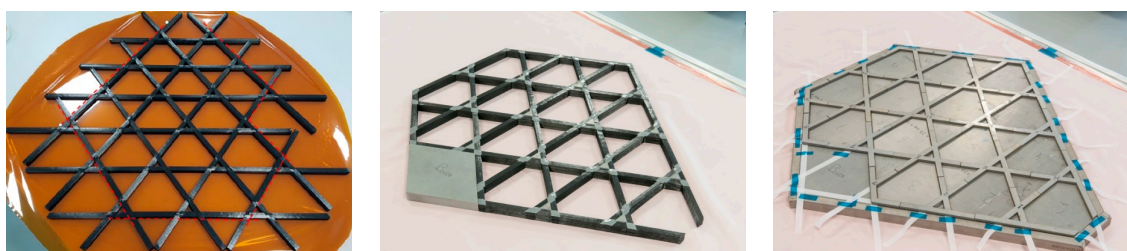


Figure 8: Fibre placement preform (left) and tooling concept (middle and right)

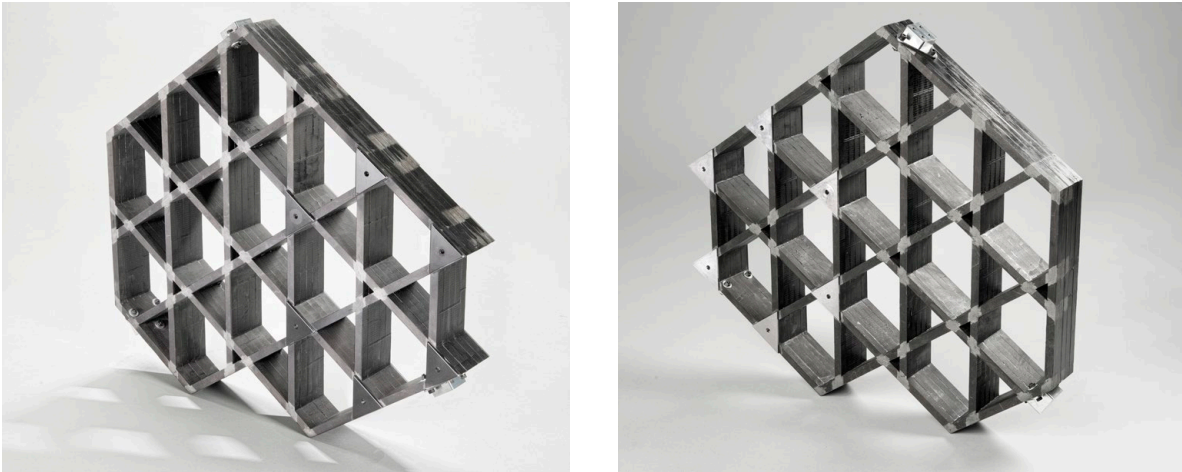


Figure 9: Final grid demonstrator (front view on the left and rear view on the right)

Due to the very high stiffness of the grid the goal was to maximize the displacements during the test for better accuracy. Therefore, the gravity release, thermal and moisture load cases were omitted as the displacements are several microns, which is very hard to measure accurately at part level, and would be better achieved at element level, with more time. The selected mechanical load cases were two loads and two moments at two single payload attachment points perpendicular to the grid. This will maximize the displacements during the test and allow for a more reliable correlation between the test results and the FEM model.

A picture of the test setup is shown in Figure 10. It consists of stiff modular steel frames bolted together creating a very stiff base structure. Load is applied using an overhead crane with a 5 kN load cell between the crane and the grid to record the load. Displacements are measured using a Digital Image Correlation (DIC) system on stickers attached to the grid and by two high accuracy mechanical displacement sensors next to the load introduction point.

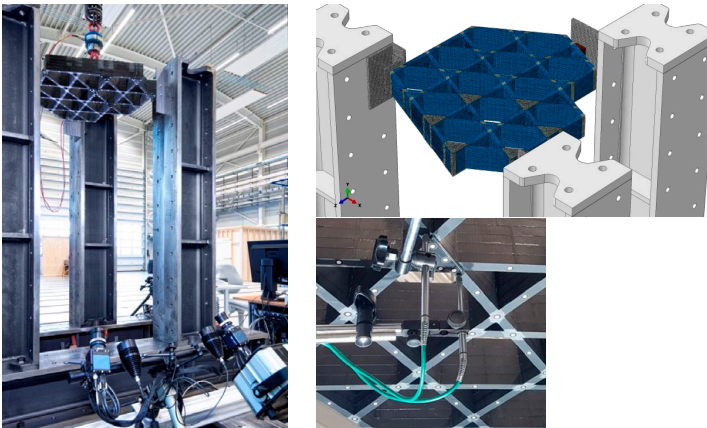
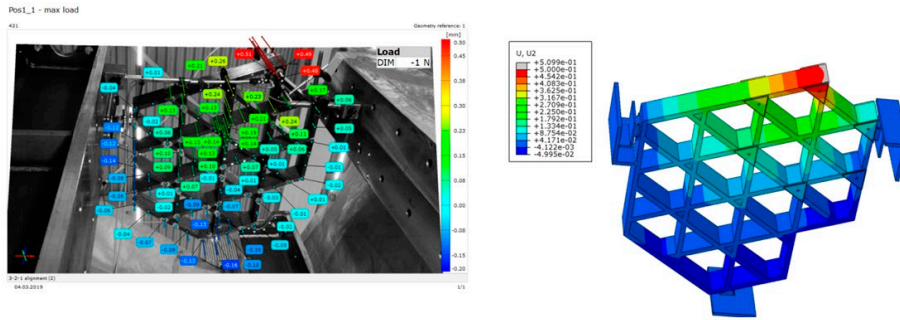
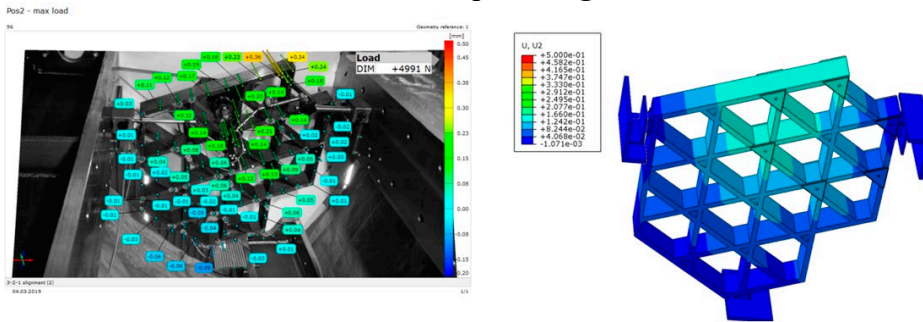


Figure 10: Test setup (left), FE model (top right) and displacement sensors (bottom right)

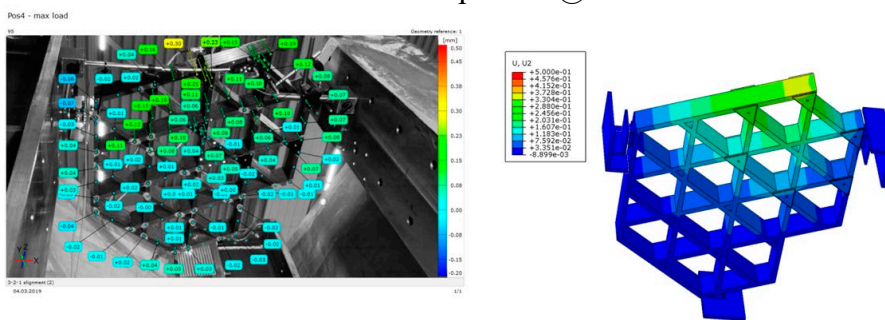
At least two runs were made for each load case to verify if the behavior of the grid is consistent. The data from the mechanical sensors was used for quantitative measurements. Unfortunately this is not the case for the optical data from the Aramis system which was not consistent and showed large scatter even at zero load. Therefore the Aramis data is only used for qualitative comparison between numerical predictions and the measured displacements. In general the Aramis data shows a similar global deformation pattern as the FE models. See next pictures for a comparison of the four tests.



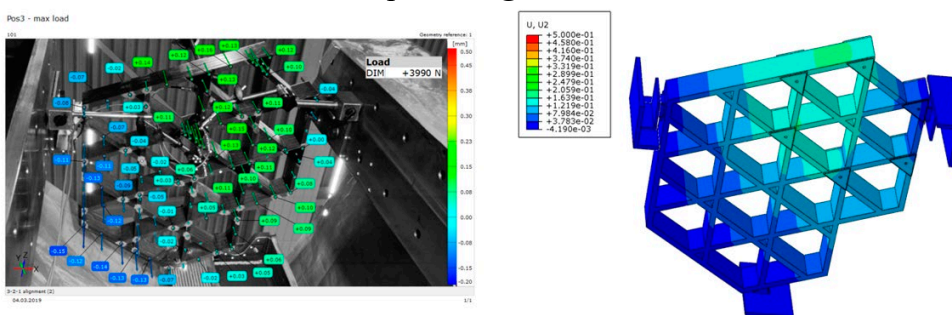
Discrete load on SWIR attachment point 1 @ 5000 N



Discrete load on SWIR attachment point 2 @ 5000 N



Moment on SWIR attachment point 1 @ 250 Nm



Moment on SWIR attachment point 2 @ 250 Nm

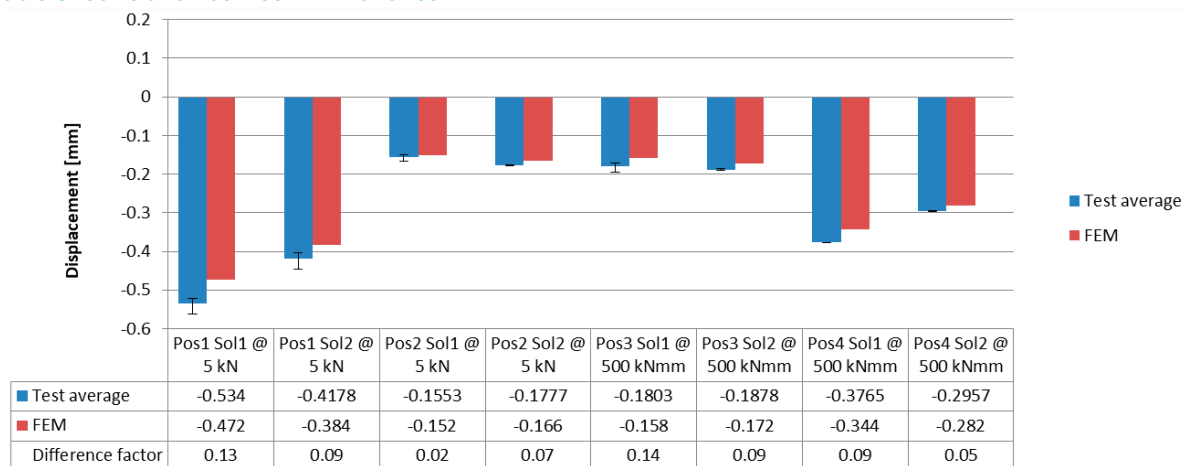
Figure 11: Comparison of global deformation pattern between Aramis data and FE model

Comparison of the measured displacements of the mechanical sensors and the predicted displacements of the FE model showed that the actual stiffness is 1 – 8 % lower than calculated in the model. In Table 3 below the correlation is shown. In two cases the grid is stiffer than predicted.

Generally the FEM displacement is lower hence the overall response as predicted is a stiffer grid than the one actually manufactured and tested. In general it can be said that the grid stiffness can be reasonably predicted by FE models however due to the small displacements

(0.5 mm maximum) the results are very sensitive to errors and accuracy of the displacement measurements during the test.

Table 3: Correlation between FEM and test



4. CONCLUSIONS

A CFRP grid structure was developed to explore the capabilities and possibilities for use in future flat support structures with high dimensional stability requirements. The final design consists of an 80 mm high anisogrid type of design which has identical crossing and close to symmetric layout with metal inserts for payload and bipod interfaces. The final weight is 13.7 kilogram. It does not meet all the stability requirements set for the gravity release load case but by using a higher grid (90 mm) or stiffer fibres this should be achievable.

Automated Fibre placement of UD prepreg tapes combination with autoclave consolidation was used to manufacture the grid. A specific cutting sequence was used for the elements and the grid to avoid local thickness increase at the crossings while still having continuous fibres across the nodes in each layer.

The correlation between FEM and test displacements was within 8 %. This demonstrates that the grid stiffness can be reasonably predicted by FE models however due to the small displacements the results are very sensitive to errors and accuracy of the displacement measurements during the test and high sensitivity towards the boundary conditions. The desired TRL level 4 has been achieved successfully. This activity demonstrates that CFRP based grid structures are a feasible solution for stable structure requirements.

5. ACKNOWLEDGEMENTS

The authors acknowledge the contribution of the ESA technical officers (Claudio Moratto, Stefan Kiryenko and Shumit Das) during the entire project and paper. Further acknowledgements go to Airbus DS NL (Javad Fatemi) for providing the case study and for their contribution to the requirement and justification deliverables and to TU Delft (Christos Kassapoglou and Dan Wang) for their work on the preliminary design activities.

6. REFERENCES

1. V.V. Vasiliev, V.A. Barynin, A.F. Razin, S.A. Petrokovskii, V.I. Khalimanovich, Anisogrid Composite Lattice Structures, Development And Space Application.

2. Nawijn, M., Design and optimisation of innovative structural components using tow placement technology (TOWOPT), NLR-CR-2012-084, March 2012.
3. E. Del Olmo, E. Grande, C.R. Samartin, Bezdenejnykh, M., Torres, J., Blanco, N., Frovel, M., Cañas, J. Lattice structures for aerospace applications. European Space Agency, (Special Publication) ESA SP. 691., 2012.
4. Niemann, S., Wagner R., Beerhorst M., Hühne C., Testing and analysis of Anisogrid Prepreg element specimens under uniaxial tension and compression, Composite Structures 160, p. 594 – 603, 24 October 2016.



Dedicated to innovation in aerospace

Royal Netherlands Aerospace Centre

NLR is a leading international research centre for aerospace. Bolstered by its multidisciplinary expertise and unrivalled research facilities, NLR provides innovative and integral solutions for the complex challenges in the aerospace sector.

NLR's activities span the full spectrum of Research Development Test & Evaluation (RDT & E). Given NLR's specialist knowledge and facilities, companies turn to NLR for validation, verification, qualification, simulation and evaluation. NLR thereby bridges the gap between research and practical applications, while working for both government and industry at home and abroad.

NLR stands for practical and innovative solutions, technical expertise and a long-term design vision. This allows NLR's cutting edge technology to find its way into successful aerospace programs of OEMs, including Airbus, Embraer and Pilatus. NLR contributes to (military) programs, such as ESA's IXV re-entry vehicle, the F-35, the Apache helicopter, and European programs, including SESAR and Clean Sky 2. Founded in 1919, and employing some 600 people, NLR achieved a turnover of 76 million euros in 2017, of which 81% derived from contract research, and the remaining from government funds.

For more information visit: www.nlr.org

Postal address

PO Box 90502
1006 BM Amsterdam, The Netherlands
e) info@nlr.nl i) www.nlr.org

NLR Amsterdam

Anthony Fokkerweg 2
1059 CM Amsterdam, The Netherlands
p) +31 88 511 3113

NLR Marknesse

Voorsterweg 31
8316 PR Marknesse, The Netherlands
p) +31 88 511 4444